The Astrophysical Journal Letters, 741:L5 (4pp), 2011 November 1 doi:10.1088/2041-8205/741/1/L5

THE CRAB NEBULA SUPER-FLARE IN 2011 APRIL: EXTREMELY FAST PARTICLE ACCELERATION AND GAMMA-RAY EMISSION

E. Striani[1], M. Tavani[1,2], G. Piano[2], I. Donnarumma[2], G. Pucella[3], V. Vittorini[2], A. Bulgarelli[4], A. Trois[2], C. Pittori[5], F. Verrecchia[5], E. Costa[2], M. Weisskopf[6], A. Tennant[6], A. Argan[2], G. Barbiellini[7], P. Caraveo[8], M Cardillo[1,2], P. W. Cattaneo[9], A. W. Chen[8,10], G. De Paris[2], E. Del Monte[2], G. Di Cocco[11], Y. Evangelista[2], A. Ferrari[10,12], M. Feroci[2], F. Fuschino[11], M. Galli[13], F. Gianotti[11], A. Giuliani[8], C. Labanti[11], I. Lapshov[2], F. Lazzarotto[2], F. Longo[7], M. Marisaldi[11], S. Mereghetti[8], A. Morselli[14], L. Pacciani[2], A. Pellizzoni[15], F. Perotti[8], P. Picozza[1,14], M. Pilia[15], M. Rapisarda[3], A. Rappoldi[9], S. Sabatini[2], P. Soffitta[2], M. Trifoglio[11], S. Vercellone[16], F. Lucarelli[5], P. Santolamazza[5], and P. Giommi[5]

[1] Dipartimento di Fisica, Universitá Tor Vergata, I-00133 Roma, Italy
[2] INAF/IASF-Roma, I-00133 Roma, Italy
[3] ENEA Frascati, I-00044 Frascati (Roma), Italy
[4] INFN-Roma La Sapienza, I-00185 Roma, Italy
[5] ASI Science Data Center, I-00044 Frascati (Roma), Italy
[6] NASA, Marshall Space Flight Center, Huntsville, AL 36812, USA
[7] Dipartimento Fisica and INFN Trieste, I-34127 Trieste, Italy
[8] INAF/IASF-Milano, I-20133 Milano, Italy
[9] INFN-Pavia, I-27100 Pavia, Italy
[10] CIFS-Torino, I-10133 Torino, Italy
[11] INAF/IASF-Bologna, I-40129 Bologna, Italy
[12] Dipartimento Fisica, Universitá di Torino, Turin, Italy
[13] ENEA-Bologna, I-40129 Bologna, Italy
[14] INFN Roma Tor Vergata, I-00133 Roma, Italy
[15] INAF-Osservatorio Astronomico di Cagliari, localita' Poggio dei Pini, strada 54, I-09012 Capoterra, Italy
[16] INAF-IASF Palermo, Palermo, Italy
[17] CNR-IMIP, Roma, Italy
[18] Dipartimento di Fisica, Universitá Dell'Insubria, I-22100 Como, Italy
Received 2011 May 24; accepted 2011 September 19; published 2011 October 7

ABSTRACT

We report on the extremely intense and fast gamma-ray flare above 100 MeV detected by *AGILE* from the Crab Nebula in mid-April 2011. This event is the fourth of a sequence of reported major gamma-ray flares produced by the Crab Nebula in the period 2007/mid-2011. These events are attributed to strong radiative and plasma instabilities in the inner Crab Nebula, and their properties are crucial for theoretical studies of fast and efficient particle acceleration up to 10^{15} eV. Here we study the very rapid flux and spectral evolution of the event that on 2011 April 16 reached the record-high peak flux of $F = (26 \pm 5) \times 10^{-6}$ photons cm^{-2} s^{-1} with a rise-time timescale that we determine to be in the range 6–10 hr. The peak flaring gamma-ray spectrum reaches a distinct maximum near 500 MeV with no substantial emission above 1 GeV. The very rapid rise time and overall evolution of the Crab Nebula flare strongly constrain the acceleration mechanisms and challenge MHD models. We briefly discuss the theoretical implications of our observations.

Key words: acceleration of particles – gamma rays: stars – pulsars: individual (Crab Nebula)

Online-only material: color figure

1. INTRODUCTION

The Crab Nebula is a most remarkable system, consisting of a rotationally powered pulsar of large spin-down luminosity ($L_{sd} \simeq 5 \times 10^{38}$ erg s^{-1}) interacting with a surrounding nebula at the center of the SN1054 supernova remnant (see, e.g., Hester 2008 for a review of Crab properties). The inner nebula is energized by the powerful wave/particle output from the pulsar, and shows distinctive optical and X-ray brightness enhancements ("wisps," "knots," and the "anvil" aligned with the pulsar "jet"; Scargle 1969; Hester et al. 1995, 2002; Hester 2008; Weisskopf et al. 2000). Despite the small-scale optical and X-ray variations detected on timescales of weeks to months, the overall high-energy flux resulting from the unpulsed synchrotron radiation of the inner nebula has been considered essentially stable for many decades.

The discovery by the *AGILE* satellite of a strong gamma-ray flare above 100 MeV from the Crab Nebula in 2010 September (Tavani et al. 2010, 2011) and the confirmation by the *Fermi* Large Area Telescope (hereafter *Fermi*-LAT; Buehler et al. 2010; Abdo et al. 2011) started a new era of investigation of the Crab Nebula and of the particle acceleration processes in general. Three intense gamma-ray flaring episodes from the Crab Nebula have been reported[19] in the gamma-ray energy range 100 MeV–a few GeV by *AGILE* and *Fermi*-LAT prior to 2011 April (Tavani et al. 2011, hereafter T11; Abdo et al. 2011, hereafter A11). This activity has been attributed to transient emission in the inner nebula due to the lack of any variation in the pulsed (radio and high-energy) signal of the Crab pulsar or of any detectable alternative counterpart (e.g., Heinke 2010; Cusumano et al. 2011).

[19] Enhanced TeV emission from the Crab Nebula has also been reported by the air-shower ARGO-YBJ (Astrophysical Radiation with Ground-based Observatory at YangBaJing) experiment in coincidence with the 2010 September event (Aielli et al. 2010). However, this claim was not supported by the simultaneous observations by VERITAS (Ong 2010) and MAGIC (Mariotti 2010).

Starting on 2011 April 11–12, a new gamma-ray flaring episode with substantial emission above 100 MeV was first detected by *Fermi*-LAT (Buehler et al. 2011; Hays et al. 2011) and then confirmed by *AGILE* (Tavani et al. 2011). The flare developed in the following days with substantial gamma-ray emission 2–3 times the normal average value[20] until on 2011 April 16 it reached the unprecedented high value of $F_\gamma = (19.6 \pm 3.7) \times 10^{-6}$ photons cm^{-2} s^{-1} for a 24 hr integration (Striani et al. 2011, hereafter F_γ is the Crab pulsar plus nebula flux above 100 MeV). This detection of very rapid variations of the gamma-ray emission in the 2011 April flare confirms a trend already noticed in the *Fermi*-LAT data for the 2010 September event by Balbo et al. (2011). A re-analysis of the 2010 September event *AGILE* data, which will be presented elsewhere, shows that the gamma-ray variability on a timescale below 1 day is confirmed also by *AGILE* for that event.

The goal of our Letter is threefold: (1) to investigate the short timescale structure of the gamma-ray emission of the 2011 April event, (2) to present the gamma-ray spectrum at the flare peak, and (3) to briefly discuss the theoretical implications of the very rapid variability and overall emission.

2. THE 2011 APRIL GAMMA-RAY SUPER-FLARE

The *AGILE* satellite (Tavani et al. 2009) has been monitoring in spinning mode[21] the Crab Nebula region with optimal exposure during the period 2011 February–April. Starting on 2011 April 10–11 a noticeable rising gamma-ray flux from a source positionally consistent with the Crab Nebula[22] was recorded by the *Fermi*-LAT instrument (Buehler et al. 2011). Enhanced emission with respect to the average flux of the steady pulsar plus nebula emission was detected at even larger flux values by *AGILE* above 100 MeV during the following days, reaching a value $F_\gamma = (6.5 \pm 1.5) \times 10^{-6}$ photons cm^{-2} s^{-1} on 2011 April 11–13 (Tavani et al. 2011). Remarkably, the gamma-ray flux increased even more in the following days, reaching the one-day averaged flux of $F_\gamma = (12.1 \pm 0.6) \times 10^{-6}$ photons cm^{-2} s^{-1} on 2011 April 14 (Hays et al. 2011), and the even larger and currently record-breaking one-day averaged flux of $F_\gamma = (19.6 \pm 3.7) \times 10^{-6}$ photons cm^{-2} s^{-1} on 2011 April 15–16 (Striani et al. 2011). Figure 1 shows the *AGILE* 12 hr binned gamma-ray light curve[23] (Crab pulsar plus nebula) during the period 2011 April 10–19 as obtained by the standard *AGILE* maximum likelihood procedure.

The 12 hr integration between MJD = 55667.0 and MJD = 55667.5 (2011 April 16) yields for the peak flux the value $F_{\gamma,P} = (26 \pm 5) \times 10^{-6}$ photons cm^{-2} s^{-1}, with a pre-trial statistical significance $\sigma_P = 10$. Considering the accumulated *AGILE* exposure on the Crab Nebula in spinning mode (equivalent to 850 maps of 12 hr integrations), the post-trial significance for the super-flare turns out to be $\sigma_{P,\mathrm{post}-t} = 9.2$. The statistical significance of this 12 hr excess emission compared to the steady Crab Nebula flux is 7.5σ. This significance is calculated by the likelihood method taking into account the standard average flux and position of the Crab pulsar and Nebula, together with the cataloged gamma-ray sources in the field. After taking into account the accumulated exposure, we find that the post-trial significance of the excess emission is 6.4σ. For a few days in 2011 April, the Crab Nebula became the brightest gamma-ray source in the sky, rivaling in intensity not only the Vela pulsar, but also the brightest blazars ever detected in gamma rays.

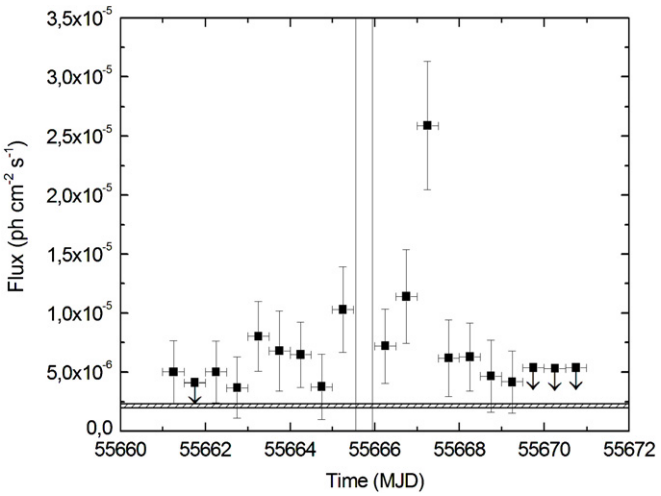

Figure 1. Crab (pulsar plus Nebula) gamma-ray 12 hr binned light curve above 100 MeV detected by *AGILE*-GRID during the period 2011 April 10–19. The gray horizontal band indicates the Crab pulsar plus nebula average flux in the *AGILE* bandpass, and the gray vertical lines mark the time period during which a loss of *AGILE*-GRID telemetry data occurred because of ground station activity. Peak emission occurred on 2011 April 16.

In order to determine the Crab super-flare peak time and duration, we proceeded as follows. Starting from the 12 hr binned light curve shown in Figure 1, we obtained different light curves by progressively shifting their bin starting times by 1 hr. These 12 light curves[24] have been compared with those calculated from a flux model obtained by integrating for each bin the model function

$$f = \begin{cases} B + Ae^{-(|t-t_P|/\sigma_r)^\nu} & \text{for } t \leqslant t_P \\ B + Ae^{-(|t-t_P|/\sigma_d)^\nu} & \text{for } t > t_P, \end{cases}$$

where $B = 1 \times 10^{-5}$ photons cm^{-2} s^{-1} day^{-1} is the flux baseline (i.e., the average of the 12 light curves baselines excluding the peak emission), t_p is the peak time, σ_r and σ_d are the rise and decay time constants, respectively, and ν is a measure of the pulse sharpness ($\nu = 1, 2$ for two-sided exponential and Gaussian fits, respectively; see, e.g., Norris et al. 1996). In general, lower values of ν imply a more peaked pulse. We also note that the rise and decay times, half to maximum amplitude, are obtained as $\tau_{r,d} = [\ln(2)]^{1/\nu}\, \sigma_{r,d}$.

In the following, we conservatively assume a Gaussian model for the flaring with $\nu = 2$ and $\sigma_r = \sigma_d$. From the values of $\sigma_{r,d}$ obtained by the best fit of each light curve (for reduced χ^2 values ranging from 1.2 to 1.4), we derived that the super-flare duration $\sigma_r + \sigma_d$ is constrained in the 68% confidence level range between 14 hr and 26 hr. Taking into account the relation $\tau_r = [\ln(2)]^{1/2}\, \sigma_r \simeq 0.8\, \sigma_r$, we obtain the rise-time range $6\,\mathrm{hr} < \tau_r < 10\,\mathrm{hr}$. This result is independent of the light

[20] The Crab steady-state (pulsar plus nebula) flux above 100 MeV detected by *AGILE* is $F_{\gamma,\mathrm{steady}} = (2.2 \pm 0.1) \times 10^{-6}$ photons cm^{-2} s^{-1}.

[21] The *AGILE* spinning mode allows a daily exposure of about 70% of the sky depending on solar panel constraints, for an instrument boresight rotation period of about 7 minutes.

[22] The possibility of a chance positional coincidence with a background transient gamma-ray source has been considered in T11 and A11. In light of the results presented also in this Letter, we consider this probability as negligible.

[23] We note that a loss of *AGILE* Gamma-Ray Imaging Detector (hereafter *AGILE*-GRID) telemetry data occurred on 2011 April 14 caused by pre-determined satellite tracking activity of the *AGILE* ground station in Malindi (Kenya). This interval partially overlaps with the first strong gamma-ray flare detected on 2011 April 14.

[24] These data points were obtained by the *AGILE* maximum likelihood procedure.

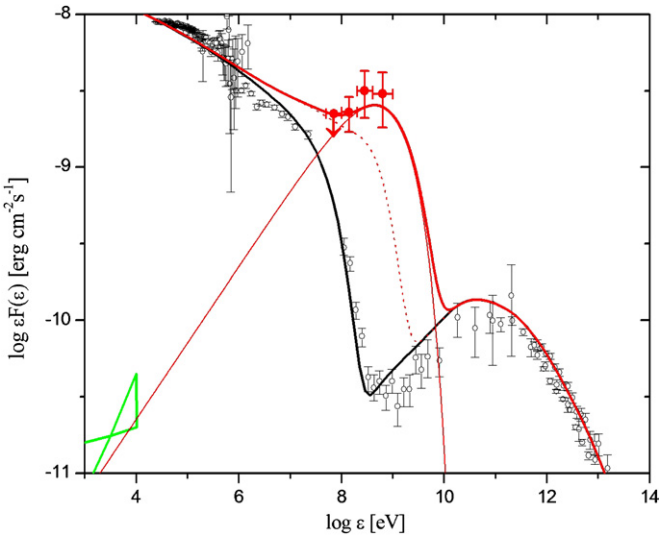

Figure 2. *AGILE*-GRID gamma-ray pulsar-subtracted spectrum of the Crab Nebula super-flare on 2011 April 15–16. The *AGILE* flaring spectral data, marked in red, obtained for a one-day integration (MJD = 245566.4–245567.4); data points marked in black show the average nebular spectrum (Meyer et al. 2010). Pulsar gamma-ray spectral data have been subtracted based on the *AGILE* results presented in Pellizzoni et al. (2009). The red curve is the result of the theoretical modeling of the super-flare as discussed in the text. The spectral region marked in green shows the X-ray spectrum of "source A" which is the most dominant source in the *Chandra* image of the "anvil" region in the inner Crab Nebula as reported in T11. This flux level is indicative of an X-ray upper bound expected from the flare.

(A color version of this figure is available in the online journal.)

curve bin zero-phase ($t_{\rm start}$) choice. The value of the peak time t_P is determined as MJD = 55667.3 ± 0.3.

A complete spectral evolution of the 2011 April event will be reported elsewhere. Here we focus on the one-day integrated 2011 April 15–16 super-flare spectrum that we show in Figure 2. Very intense and relatively hard emission is detected in the energy range 100 MeV–1 GeV. The *AGILE* optimal spectral sensitivity in the 50 MeV–a few GeV energy range is important in constraining the spectrum at relatively low gamma-ray energies. Indeed, the 50–100 MeV flux is well constrained by our 95% confidence level upper limit. The super-flare emission shows a very prominent peak of the νF_ν spectrum at photon energies $E_{\gamma,P} \simeq 500$ MeV. No significant emission is detected above 1 GeV.

Figure 2 shows also the results of our theoretical modeling of the emission (red curve) that we discuss below. Remarkably, the peak power emitted in the gamma-ray energy range between 100 MeV and a few hundreds of MeV equals the average power emitted in the hard X-ray/MeV energy range by the Crab Nebula.

3. THEORETICAL CONSTRAINTS

In modeling the 2011 April Crab Nebula gamma-ray event we assume that fast and very efficient acceleration is occurring at a site in the inner nebula, following the discussion of T11 and Vittorini et al. (2011, hereafter V11). A fraction of the total electron–positron high-energy component in the Nebula is impulsively accelerated at a site of size L. For simplicity, we ignore here substantial enhancements due to Doppler boosting and take the Doppler factor $\delta = \Gamma^{-1}(1-\beta\cos\theta)^{-1}$ to be of the order of a few.

The physical quantities are constrained within a global comparison of a multi-parameter model matching spectral and timing data.[25] We considered several models with the assumption of δ in the range 1–4 as deduced from observations of the southeast jet and wisp regions (e.g., Hester 2008). We present here the cases with $\delta = 1$ and $\delta = 4$ as examples of a class of models applied to the super-flare spectrum shown in Figure 2.

The acceleration process produces, within a timescale shorter than any other relevant timescale, a differential particle energy distribution (that we model for illustration purposes in its simplest form as a single power-law distribution $dn/d\gamma = K\,\gamma_b^{-1}/(\gamma/\gamma_b)^s$, where n is the local particle number density, γ is the particle Lorentz factor ranging from $\gamma_{\rm min} = 10^5$ to $\gamma_{\rm max} = 7\times10^9$, $s = 2$ is the power-law index, $\gamma_b = 5\times10^8$, and K is the normalization factor $K = 4\times10^{-7}$ cm^{-3}. For $\delta = 1$, the emitting region has size $L = 10^{15}$ cm, and an enhanced local magnetic field $B_{\rm loc} = 2\times10^{-3}$ G that we keep constant in our calculations. The total particle number required to explain the flaring episode turns out to be $N_{e-/e+} = \int dV\,(dn/d\gamma)\,d\gamma \simeq 7\times10^{42}$, where V is an assumed spherical volume of radius L. For $\delta = 4$, some of the physical parameters are slightly different, e.g., $\gamma_{\rm max} = 5\times10^9$, $B_{\rm loc} = 1.3\times10^{-3}$ G, $K = 3\times10^{-10}$ cm^{-3}, $L = 4\times10^{15}$ cm, and $N_{e-/e+} = 3\times10^{41}$. Obviously, the physical parameters can differ from these (and are even more extreme) for time variations faster than the one-day spectral average of Figure 2. A discussion of the complete light curve and physical implications will appear elsewhere. The complex gamma-ray light curve shows that the acceleration process occurs on a ∼week timescale with a succession of short timescale flares, each of which has physical parameters which differ from those of the peak emission by a factor of a few.

We find that the synchrotron peak photon energy during the flare maximum is $E_{\rm peak} = \frac{3}{2}\hbar\,\frac{e\,B_{\rm loc}}{m_e\,c}\,\gamma_{\rm max}^2 \simeq 500$ MeV, a value that challenges models of diffusive particle acceleration limited by synchrotron cooling, a fact already noticed in T11, A11, and V11. The 2011 April event confirms even more the extremely short timescale of acceleration occurring in the inner Crab Nebula and the existence of a strongly enhanced local magnetic field.

4. DISCUSSION AND CONCLUSIONS

The 2011 April Crab Nebula super-flare dramatically shows the efficiency of the particle acceleration mechanism operating in the inner nebula. The detected gamma-ray luminosity at the peak of the 2011 April 16 super-flare corresponds to 0.3% of the Crab pulsar spin-down luminosity. Despite recent high-resolution observations of the inner nebula (see especially the very interesting sequence of *Chandra* pointings reported by Tennant et al. 2011), there is currently no identification of the acceleration site. The anvil region has been suggested as a candidate for the 2010 September event (T11), and this site may well be active also in the case of the 2011 April event.

[25] Having determined from the overall spectral shape the values of γ_b and index s (see their definitions in the text), we have five remaining parameters: $\gamma_{\rm max}$, the local magnetic field B, the electron density N_e, the dimension of the emitting region L, and the Doppler factor δ (the parameter K is derived from N_e and L). These parameters are obtained from the following quantities (in the observer frame): the position of the peak emission, $E_p \propto \delta\,\gamma_{\rm max}^2\,B$, the peak emission $\nu F \propto \delta^4\,N_e\,L^3\,B^2\,\gamma_{\rm max}^2$, the rise time $\tau_r = L/(c\,\delta)$, and the cooling time $\tau_c \propto 1/(B_{\rm loc}^2\,\gamma_{\rm max}\,\delta)$.

More observations and extended monitoring of the Crab Nebula are necessary also in light of the "secular" X-ray variations as determined over a timescale of years (Wilson-Hodge et al. 2011).

The challenge to particle acceleration models applies to the main theoretical frameworks that have been so far proposed for the Crab Nebula: the magnetohydrodynamical approach of Kennel & Coroniti (1984), diffusive shock acceleration mechanisms (e.g., Drury 1983; Blandford & Eichler 1987), shock drift acceleration (e.g., Kirk et al. 2000; Reville & Kirk 2010), magnetohydrodynamical instabilities (e.g., Komissarov & Lyubarsky 2004; Del Zanna et al. 2004; Camus et al. 2009; Komissarov & Lyutikov 2010), and ion-driven acceleration (e.g., Arons 2008). The data presented here contribute in a substantial way to a step further in deepening our understanding of acceleration processes and may force the previously proposed models to be substantially revised. Of particular relevance is the possible role of impulsive particle acceleration in magnetic field reconnection, and/or runaway particle acceleration by transient electric fields violating the condition $E/B < 1$ (that is typically assumed in standard models, e.g., de Jager et al. 1996). The super-flare spectrum of Figure 2, showing significant emission above 200 MeV, implies $E/B \geqslant 2$ (Tavani 2011). The applicability of these concepts to the Crab Nebula flaring activity remains to be tested by future investigations.

Research partially supported by ASI grant No. I/042/10/0.

REFERENCES

Abdo, A. A., Ackermann, M., Ajello, M., et al. 2011, Science, 331, 739 (A11)
Aielli, G., Patruno, A., Watts, A., et al. 2010, ATel, 2691
Arons, J. 2008, in Neutron Stars and Pulsars, 40 Years After the Discovery, ed. W. Becker & H. H. Huang (MPE Rep. 291; Garching: MPE), arXiv:0708.1050
Balbo, M., Walter, R., Ferrigno, C., & Bordas, P. 2011, A&A, 527, L4
Blandford, R., & Eichler, D. 1987, Phys. Rep., 154, 1
Buehler, R., D'Ammando, F., & Cannon, A. 2011, ATel, 3276
Buehler, R., D'Ammando, F., & Hays, E. 2010, ATel, 2861
Camus, N. F., Komissarov, S. S., Bucciantini, N., & Hughes, P. A. 2009, MNRAS, 400, 1241
Cusumano, G., Parola, V. La., Romano, P., Burrows, D. N., & Gelbord, J. M. 2011, ATel, 3279
de Jager, O. C., Harding, A. K., Michelson, P. F., et al. 1996, ApJ, 457, 253
Del Zanna, L., Amato, E., & Bucciantini, N. 2004, A&A, 421, 1063
Drury, L. O. 1983, Rep. Prog. Phys., 46, 973
Hays, E., Buehler, R., & D'Ammando, F. 2011, ATel, 3284
Heinke, C. O. 2010, ATel, 2868
Hester, J. J. 2008, ARA&A, 46, 127
Hester, J. J., Mori, K., Burrows, D., et al. 2002, ApJ, 577, L49
Hester, J. J., Scowen, P. A., Sankrit, R., et al. 1995, ApJ, 448, 240
Kennel, C. F., & Coroniti, F. C. 1984, ApJ, 283, 710
Kirk, J. G., Guthmann, A. W., Gallant, Y. A., & Achterberg, A. 2000, ApJ, 542, 235
Komissarov, S. S., & Lyubarsky, Y. E. 2004, MNRAS, 349, 779
Komissarov, S. S., & Lyutikov, M. 2010, MNRAS, 414, 2017
Mariotti, M. 2010, ATel, 2967
Meyer, M., Horns, D., & Zechlin, H. S. 2010, A&A, 523, A2
Norris, J. P., Nemiroff, R. J., Bonnell, J. T., et al. 1996, ApJ, 459, 393
Ong, R. A. 2010, ATel, 2968
Pellizzoni, A., Pilia, M., Possenti, A., et al. 2009, ApJ, 691, 1618
Reville, B., & Kirk, J. G. 2010, ApJ, 724, 1283
Scargle, J. D. 1969, ApJ, 156, 401
Striani, E., Piano, G., Tavani, M., et al. 2011, ATel, 3286
Tavani, M. 2011, in Proc. 25th Texas Symp. on Relativistic Atrophysics, December 06–10 2010, Heidelberg, Germany (arXiv:1106.0164v2)
Tavani, M., Barbiellini, G., Argan, A., et al. 2009, A&A, 502, 995
Tavani, M., Bulgarelli, A., Striani, E., et al. 2011, ATel, 3282
Tavani, M., Bulgarelli, A., Vittorini, V., et al. 2011, Science, 331, 736 (T11)
Tavani, M., Striani, E., Bulgarelli, A., et al. 2010, ATel, 2855
Tennant, A., Blandford, R., Buehler, R., et al. 2011, ATel, 3283
Vittorini, V., Tavani, M., Pucella, G., et al. 2011, ApJ, 732, L22 (V11)
Weisskopf, M. C., Hester, J. J., Tennant, A. F., et al. 2000, ApJ, 536, L81
Wilson-Hodge, C. A., Cherry, M. L., Case, G. L., et al. 2011, ApJ, 727, L40